PAPER

A novel mid-infrared thermal emitter with ultra-narrow bandwidth and large spectral tunability based on the bound state in the continuum

IOP Publishing Journal of Physics D: Applied Physics
J. Phys. D: Appl. Phys. **55** (2022) 025104 (7pp) https://doi.org/10.1088/1361-6463/ac2a78

A novel mid-infrared thermal emitter with ultra-narrow bandwidth and large spectral tunability based on the bound state in the continuum

Kaili Sun[1], **Yangjian Cai**[1,2] **and Zhanghua Han**[1,*]

[1] Shandong Provincial Key Laboratory of Optics and Photonic Devices, Center of Light Manipulation and applications, School of Physics and Electronics, Shandong Normal University, Jinan 250358, People's Republic of China
[2] School of Physical Science and Technology, Soochow University, Suzhou 215006, People's Republic of China

E-mail: zhan@sdnu.edu.cn

Received 14 August 2021, revised 16 September 2021
Accepted for publication 27 September 2021
Published 11 October 2021

Abstract

The development of efficient, compact and low-cost mid-infrared (MIR) sources with easy manufacturing is vital in a variety of applications including gas sensing, thermal photovoltaic power generation, infrared imaging, among others. In this work, we demonstrate that a novel type of MIR thermal emitters with ultra-narrow bandwidth and broad spectral tunability can be realized based on a new operation principle employing the concept of bound state in the continuum (BIC). Using an elaborately designed structure composed of two interdigitated gratings with the same pitch and different stripe width on a slab supported by a conducting substrate, the quasi-BIC mode with both ultra-high Q-factor ($>10^4$) and large absorbance/emittance can be achieved, resulting from the destructive interference between the couplings of two guided-mode resonances back to free space. At the operation wavelength of 7.7851 μm, even when the metal dissipation is considered, a near-unity emission at resonance with the full-width at half-maximum less than 0.3 nm is numerically presented, which is three orders of magnitude narrower than conventional metallic metamaterial based thermal emitters. By applying a geometrical scaling of the structure, the operation wavelength can be flexibly extended to other wavelengths of the MIR region. The presented novel thermal emitter with economic advantages and high performances of both ultra-narrow bandwidth and broad wavelength-tunability, will make great impact in practical applications.

Keywords: mid-infrared, thermal emitter, ultra-narrow bandwidth

(Some figures may appear in colour only in the online journal)

* Author to whom any correspondence should be addressed.

1. Introduction

The mid-infrared (MIR) is widely recognized as the molecular fingerprint region because the vibration resonances of many chemicals fall well into this band. The spectroscopic information in this region is particularly useful for the identification of certain intra-molecule chemical bonds, as opposed to terahertz spectroscopy techniques which are more suitable for inter-molecule resonances like hydrogen bonds. Thus, the MIR technology is of vital importance for a variety of applications spanning from environmental gas sensing [1, 2], biomedical diagnosis [3, 4], to hyperspectral imaging [5, 6] and industrial process control [7], etc.

In real applications especially for commercialization, cost-effective sensing systems with acceptable sensitivity and high compactness is preferred, thus the use of bulky and expensive spectroscopic devices is usually excluded. The approach of non-dispersive infrared (NDIR) [8] system is more generally adopted when the target chemical is specified beforehand and its characteristic absorption wavelengths in the mid-IR are known. The NDIR system will identify whether the target chemical exists and, if it does, makes a quantitative measurement according to Beer–Lambert law. One typical configuration of the NDIR system is to use a blackbody thermal emitter and a MIR detector, which both have broadband responses. A band-pass filter usually composed of multilayer dielectric structures with a narrow response is applied before the detector so that only the signal at the target characteristic wavelength will be measured. For the detection of more-than-one substances, multiple filters are needed with additional installation apparatus by using e.g. a rotating wheel, and special attention is required to eliminate possible spectral interference, making the system more complicated and time-consuming during the measurement. To address this problem, Tan *et al* incorporated a nanoantenna-based narrowband absorber array into a single pyroelectric detector and achieved multi-gas sensing with a regular IR source [9]. Another configuration of the NDIR system is to use a narrowband IR emitter and then the requirement of the band-pass filter is eliminated. Because the absorption linewidths of many substances, especially gases, are very narrow, stringent requirement is posed for the MIR emitter to have adequately narrow bandwidth so that the spectral information of the target substance can be fully resolved. Other attributes of the MIR emitters include large spectral tunability for the identification of different target chemicals on the same platform, low cost and low power consumption, adequate compactness for easy instrumentation, and ease of operation in ambient conditions. Although various narrowband continuous-wave IR sources have been developed to date, including MIR quantum cascade laser [10], interband cascade laser [11], free-electron laser [12], they are not suitable for NDIR applications because one or more of the above requirements cannot be fulfilled.

For economical consideration, the most suitable way of generating MIR radiations is still to use the ubiquitous blackbody thermal emitter, which can generate thermal radiation only by heating the object structure. However, according to Planck's law, the spectrum of radiations from the thermal emitter is usually very broad, and its emissivity and emission peak are determined by the heating temperature. Nevertheless, it is still possible to incorporate artificial structures into thermal emitters to engineer the emission properties [13]. In that case, both the emission bandwidth and the emissivity of the whole emitter will be determined not by the temperature but by the nature of the structure. To this end, researchers have made quite a lot of efforts to use artificial structures or in other words metamaterials to realize narrowband and tunable MIR thermal emitters. Various schemes on different material platforms have been demonstrated to achieve thermal emitters that exhibit relatively narrow bandwidth at the target wavelength, including metallic sandwich structures in the form of metal–insulator-metal configuration [14], dielectric photonic crystals [15], semiconductor quantum well structures [16]. New physics and mechanisms have also been exploited for the same purpose, including the surface phonon polarization supported by SiC gratings [17] or the moiré effect in a twisted two-grating structure above a tungsten substrate [18]. In addition, some researchers have introduced the phase change materials like VO_x [19] or $Ge_2Sb_2Te_5$ [20] to adjust their dielectric constants by changing the temperature. Although the above methods and structures have been intensively exploited, their emission peaks are still not narrow enough. Furthermore, for NDIR applications, the target substance is usually prespecified and the characteristic absorption wavelength is fixed. So a dynamic or active control of the peak emission wavelength is an asset but not essential, as long as one can tune the peak emission wavelength to match the target substance by e.g. geometrical changes. In general, the pursuing of a simple and efficient MIR source with ultra-narrow bandwidth and large spectral feasibility is still a constant research goal.

In this paper, we propose a novel type of MIR thermal emitter with ultra-narrow bandwidth by employing the new physics of bound state in the continuum (BIC). The concept of BIC was first proposed by Friedrich and Wintgen in quantum mechanics [21], and then was introduced to acoustics [22], electrodynamics [23], and photonics [24] in recent years. The BIC resonance is achieved in our work by manipulating two guided mode resonances (GMRs) supported by a slab waveguide and a special type of interdigitated gratings composed of two ridge gratings with the same pitch and different stripe width, placed on a conducting substrate. Both the two layers are made from the same refractory material of Al_2O_3 due to its negligible material loss in the MIR range. By elaborately designing the structure, it supports a sharp resonance in the reflection spectrum due to the excitation of a quasi-BIC mode. According to Kirchhoff's law of thermal radiation, the emissions from the structure after applying high temperatures have the same electromagnetic characteristics as the absorptivity. Our numerical results demonstrate that an emission bandwidth less than 0.3 nm can be achieved at the wavelength of 7.7851 μm even when all the material absorptions are considered. By applying a geometrical scaling of the whole structure, the advantages of near-unity emissivity

and ultra-narrow bandwidth can be easily extended to a large wavelength range. Our results reveal that the emission can be tuned across the range of 3.6–8 μm, well below the phonon resonance of the Al_2O_3 material. Although many methods have been attempted to achieve narrowband MIR thermal emitters, our proposed BIC based thermal emitter outperforms others by further reducing the bandwidth. Besides the high monochromaticity, this type of emitter has additional advantages of high directionality and linearly polarization. Therefore, it represents a new approach to realize efficient MIR sources and may find significant applications in NDIR sensing systems.

2. Structure and results

The structure of the BIC-based MIR thermal emitter is schematically depicted in figure 1(a), and is composed of an interdigitated grating composed of two alternatingly aligned ridge gratings with the same pitch and different stripe width separated from the conducting substrate by a waveguiding layer. The whole structure is assumed invariant in the z-direction and the period $P = 6$ μm in the x-direction. The yellow region represents the gold substrate, and its relative permittivity can be defined by the Drude–Lorentz dispersion model [25]:

$$\varepsilon(\omega) = \varepsilon_\infty - \frac{\omega_p^2}{\omega^2 + i\gamma\omega}$$

where ω is the angular frequency, $\varepsilon_\infty = 1$, the plasma frequency ω_p and damping constant γ are 1.37×10^{16} rad s^{-1} and 4.08×10^{13} rad s^{-1} respectively. The blue region represents the grating and waveguiding layers and they are both made from the refractory material of Al_2O_3, whose refractive index is given by the tabulated experimental results [26]. The thickness is $h_1 = 4.5$ μm for the grating layer and $h_2 = 5.9$ μm for the waveguiding layer. As shown in figure 1(b), in the same unit cell, the width of two ridges is different, where one is $w = 1.5$ μm and the other is increased by $\delta = 0.1$ μm. When a plane wave is incident onto the periodic structure, one grating will couple the light into a guided mode supported by the three-layer air-Al_2O_3–Au geometry at the wavelength where the phase matching condition is fulfilled. This guided mode will propagate laterally and then couple back to free space due to the infinite distribution of the same excitation grating, giving rise to the phenomenon of GMR in the reflection spectrum. Since the two ridge gratings have the same period, they correspond to the same guided mode wavelength. However, the slight deviation of the grating width results in a different coupling efficiency (particularly in the phase) to free space from the two GMRs. In principle, an ideal BIC resonance will then be formed with an infinite quality factor when δ shrinks to 0. However, in that case, the BIC mode cannot be excited by a plane wave since its coupling channel to the external environment is closed. When a slight deviation is introduced intentionally between the two grating element width, a quasi-BIC mode will be preserved, manifesting itself as a reflection dip with a non-infinite but still ultra-high (>10^4) quality factor. Because the metal substrate is thick enough, the transmissivity vanishes in the whole MIR regime, so the reflection dip corresponds to a strong absorption. Based on Kirchhoff's law of thermal radiation [27], for any object in the thermodynamic equilibrium, the process of thermal emission is reciprocal to the absorption. The yellow arrows and red output beam in figure 1(a) schematically demonstrate the upward thermal radiation generated by heating the whole structure by applying an electric current. Note that only the emission at TE polarization is considered in this work, which corresponds to the electric field along the z direction in both the structure and free space. However, since the waveguiding layer supports both guided mode of the TE and TM types, all the obtained results can be easily extended to the TM case.

We use the finite element method implemented in the software of COMSOL Multiphysics to investigate the dispersion characteristic. By establishing a 2D model with the unit cell shown in figure 1(b), and applying the Floquet periodic boundary conditions in the x direction to account for the lateral wave vector, the eigen frequencies supported by the structures are calculated. The solid blue line in figure 2(a) presents the calculated resonances while the light dispersion in free space is also given as the black dotted line. Apparently, the resonances are located above the light line, i.e. within the radiation continuum region, indicating the resonances supported by the structure belongs to the category of BIC. One can also see that even when a conducting substrate is present, the resonance is weakly affected by the lateral wave vector, which is consistent with the results supported by all-dielectric structures [28]. It is plotted in figure 2(b) the resonance wavelength and Q-factor with respect to the lateral wave vector respectively. As the wave vector increases, the Q-factor experiences first a slight decrease and then increases. The non-monotonic behavior of the Q-factor as a function of lateral wave vector is attributed to the material dispersion of the Al_2O_3, which has been fully considered in the calculations. In general, the Q-factor is at the order of 10^4. Particularly, when the wave vector is zero, which corresponds to the emission in the normal direction, the Q-factor is above 3.6×10^4. This suggest that a thermal emitter with ultra-narrow bandwidth can be realized. We note that all these results are achieved by assuming the grating width difference as $\delta = 0.1$ μm. The Q-factors can be actually further increased by reducing the value of δ, as shown in figure 2(c). When δ is zero, the Q-factor approaches infinity as in the case of an ideal BIC, limited only by the loss of the metal substrate. A value of $\delta = 0.1$ μm will ensure the structure can be steadily fabricated by standard processes while maintaining a finite yet ultra-high Q-factor.

The electromagnetic characteristics of the two processes of absorption and emission, including the frequency and polarization, are the same while the direction of power propagation is opposite. Therefore, to investigate the emission property of a structure, one only needs to study the absorption of it instead, which is a common approach of studying thermal emitters. According to energy reservation, the absorption $A(\omega) = 1 - T(\omega) - R(\omega)$, where $T(\omega)$ and $R(\omega)$ represent the transmissivity and reflectivity respectively. Since

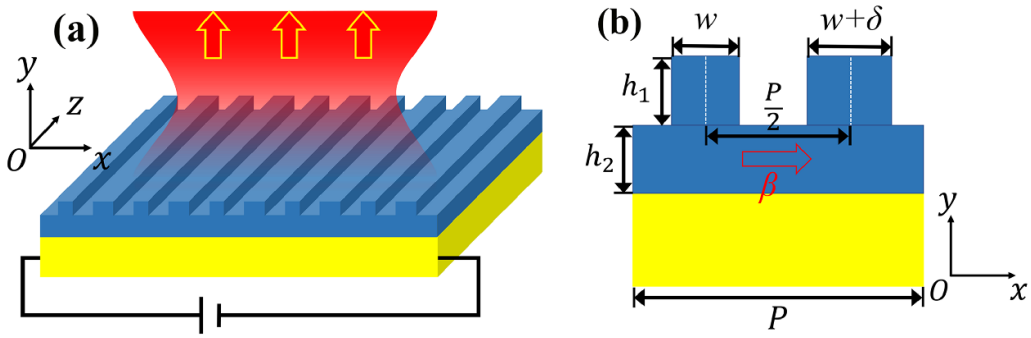

Figure 1. (a) Schematic model of the novel thermal emitter based on the BIC resonance supported by the interdigitated grating-waveguiding structure. The red output beam represents the thermal radiation at BIC resonance. (b) The cross sectional view of a single unit cell of the structure.

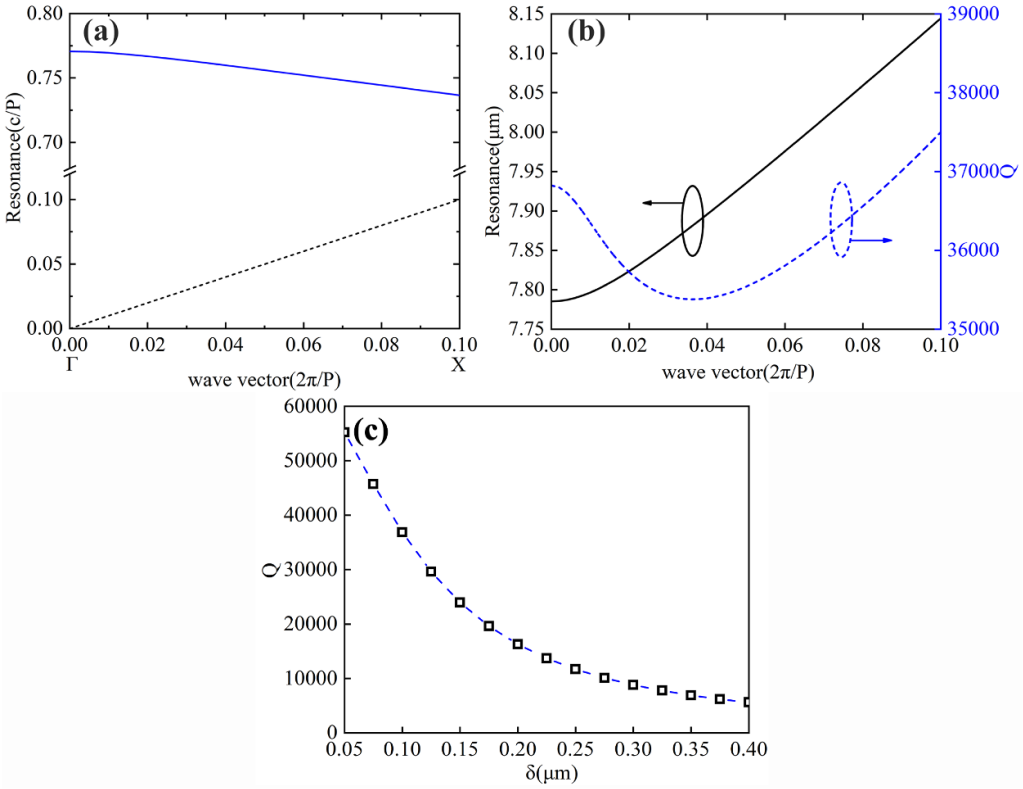

Figure 2. (a) The band structure of the quasi-BIC mode supported by the interdigitated grating-waveguiding structure. The blue solid line represents the supported resonance, while the dotted line is for light in free space. (b) Dependence of the quasi-BIC wavelength and the resonance Q-factor as a function of the lateral wave vector, respectively. (c) Dependence of Q-factor on δ, and the dash line is a fitting of the results.

the gold substrate is thick enough, the transmissivity diminishes to 0 and one can simply calculate the emissivity by $E(\omega) = 1-R(\omega)$. Figure 3(a) presents the calculated emission spectrum using this approach of the investigated structure along normal output direction at TE polarization. It is obvious that the structure has two emission peaks in the range of 7.2–8.8 μm, where the one around 7.8 μm has a near-unity emissivity while the other one around 7.4 μm is much weaker. The inset of figure 3(a) gives an enlarged picture of the first resonance and demonstrates an emission bandwidth of less than 0.3 nm at the wavelength of 7.7851 μm, which corresponds to a Q factor at the order of 10^4. This narrow bandwidth is 3 orders of magnitude smaller than that from metal metamaterials [14, 29]. Figure 3(b) shows the electric field distribution at the resonance wavelength of 7.7851 μm and one can clearly observe within the waveguiding layer an anti-symmetric profile of the E field. This field distribution suggests that the quasi-BIC resonance at normal incidence can be considered as the symmetry-protected type of BIC because of the incompatibility of the field distribution with that of a plane wave. The field distribution also indicates that the GMR is due to the excitation of the TE_0 mode in the waveguiding layer. The second

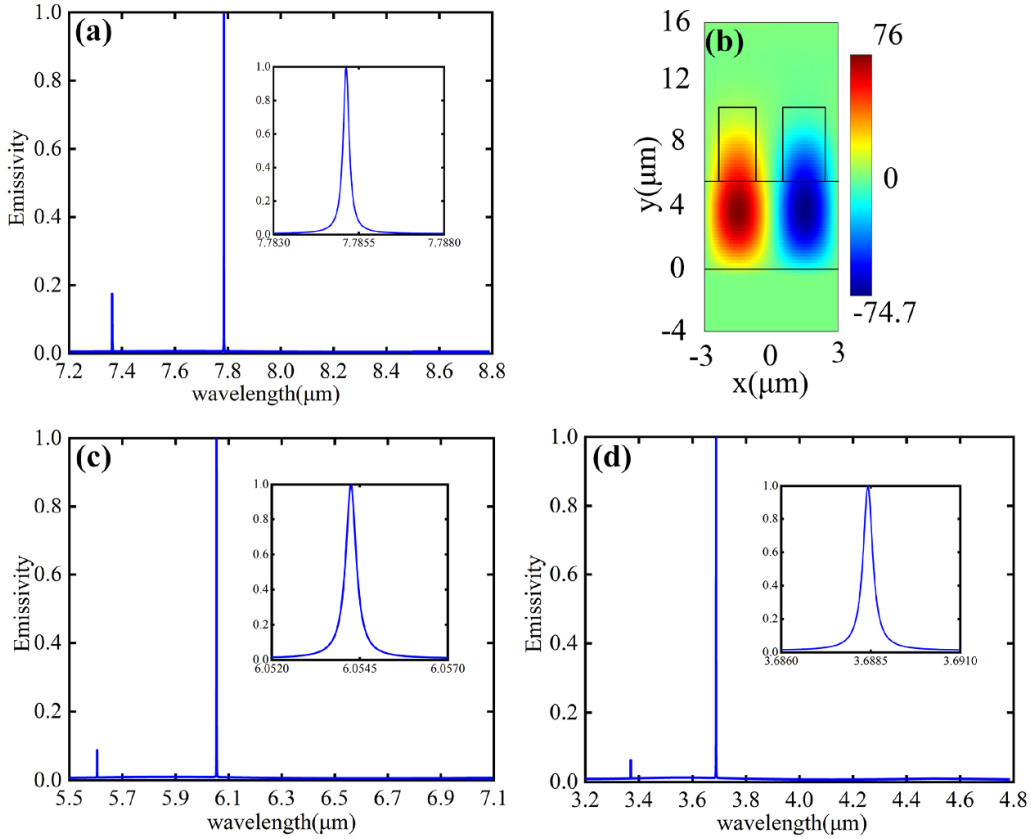

Figure 3. (a) Spectrum of emission at TE-polarization from the interdigitated grating-waveguiding structure along normal direction; the inset is an enlarged view of the emission peak. (b) The distribution of the real part of E_z on resonance in the xy plane. (c) and (d) present the emission spectra of the structure scaled by a factor of 0.7 and 0.4 respectively, both calculated along normal direction and at TE-polarization.

emission peak has an emissivity less than 0.2, and this peak is attributed to the excitation of a higher order of the guided mode. Since there is a large spectral gap (∼400 nm) between the two emission peaks, the second emission will not cause significant spectral interference to the first one in the NDIR applications.

One additional asset of the design is that the geometry can be scaled so that the emission wavelength can be extended easily within the MIR range. To demonstrate this point, we plot in figures 3(c) and (d) the emission spectrum which corresponds to the two cases where the above structure is scaled by a factor of 0.7 and 0.4 respectively. It can be clearly seen that the original emission peak at 7.7851 μm in figure 3(a) shifts to 6.0543 μm and 3.6884 μm respectively, however, both still with near-unity emissivity and the Q-factors at the order of 10^4. The working band of this novel MIR thermal emitter can be further adjusted by using a larger scaling factor, and the covering of the whole range between 3 and 8 μm below the phonon resonance of Al_2O_3 can be realized. Since similar structure array with different scaling factors can be easily integrated on a same chip [30, 31], one can expect to achieve a thermal emitter array with multiple emission wavelengths, all with ultra-narrow bandwidth but corresponding to the characteristic absorption wavelengths for different target substances. Then the NDIR sensing of multiple specimen can be realized during a single measurement without the requirement of complicated band-pass filters or expensive spectroscopic component.

In addition to the narrow bandwidth, broad wavelength-tunability on the same platform, and linear polarization characteristics of this MIR thermal emitter, we further show that it has a superior emission directionality. Taking the original structure which has a peak emission wavelength of 7.7851 μm as an example, the emissivity at different output angle is evaluated according to Kirchhoff's law of thermal radiation, by calculating the structure absorptivity of a TE-polarized plane wave at different incident angles. Figure 4(b) shows the dependence of emissivity on the output angle when the output wavelength is fixed at 7.7851 μm. It can be seen that the emissivity decreases sharply from 1 in the normal direction to 0 at an inclination of 0.3°, which shows a highly directionality performance of the emitter. For a larger output angle, the central emission wavelength also experiences a red-shift, which is accompanied with a gradual decrease of the emissivity. The emission spectra at different output angles are presented in figure 4(a) and the results are consistent with those in figure 2(b) that a larger resonance wavelength is associated with an increased lateral wave vector. The overall ultrahigh Q-factors in figure 2(b) at different lateral wave vector also suggests that the emission bandwidth will keep

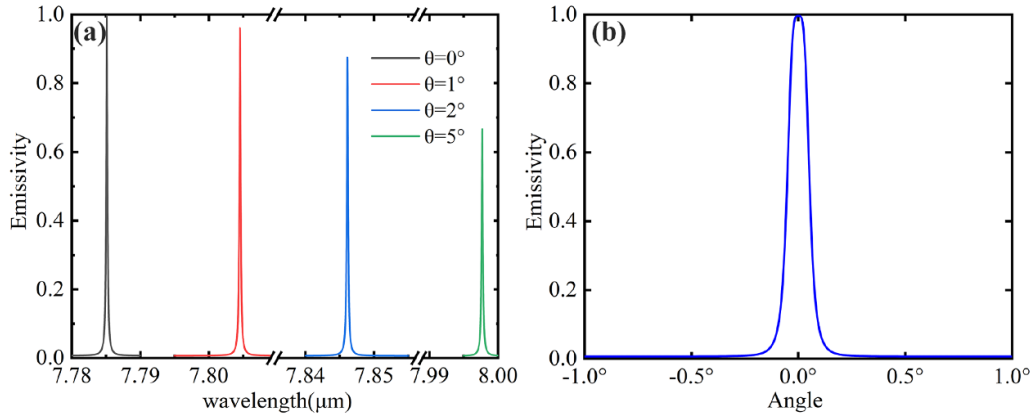

Figure 4. (a) Emission spectrum of the interdigitated grating-waveguiding structure at different output angles. (b) The dependence of the emissivity on the output angle at the wavelength of 7.7851 μm.

the ultra-narrow characteristics. This is verified in figure 4(a) where one can see that the narrow bandwidth remains almost the same. The results in figure 4(a) demonstrate that when the thermal emitter is heated to a high temperature, actually a broadband of emission is present with a special property that each emitted wavelength corresponds to a certain emission angle, around which the emission at this wavelength possesses a sharp angular distribution. However, each structure has its own characteristic emission wavelength at which the normal emission is present. This kind of rainbow behavior has also been found in other types of thermal emitter [17]. In practice, one can use a spatial filter to retract the wavelength of emission of his own interest.

The quasi-BIC modes presented in figure 4(a) in both the normal and inclined directions raise the question about the origin of the quasi-BIC resonances supported by the interdigitated grating structure on a slab investigated in our work. In the normal direction, the anti-symmetric profile of the electric field in figure 3(b) suggests that it belongs to the symmetry-protected type of BIC due to the incompatibility of the electric field to that of a plane wave. However, this is not true for the inclined directions where the symmetry is not limiting. Our further calculations also reveal that the quasi-BIC resonances in the inclined directions do not belong to Friedrich-Wintgen type [32] as well, because we have not observed the avoided crossing phenomenon of resonances in a 2D mapping of the incident angle and the wavelength. Actually two resonances at different wavelength usually exist in the Friedrich-Wintgen BIC. In our case of the interdigitated grating, since it is composed of two alternatingly aligned ridge gratings with the same pitch but different width, two GMRs are present at roughly the identical wavelength. However, the coupling coefficient in the two GMRs have different or opposite phases at certain wavelengths, so there will be a destructive interference between the two GMRs coupling back to free space, leading to an elimination (for the ideal BIC) or narrowing (for the quasi-BIC) of the original GMR resonance. We believe that the quasi-BICs in the normal and the inclined directions can both be attributed to the destructive interference between the coupling of the two GMRs to free space.

3. Discussions and conclusion

In a summary, we have demonstrated in this work a novel type of thermal emitter working in the MIR with ultra-narrow bandwidth and broad wavelength-tunability, based on the new physics of BIC. By using an interdigitated grating-waveguiding structure on a conducting substrate, a quasi-BIC mode similar to that supported by all-dielectric nanostructures can be achieved thanks to the low dissipation loss of novel metals in the MIR, leading to a sharp absorptivity/emission resonance with ultra-narrow bandwidth. We numerically show that at the thermal emission wavelength of 7.7851 μm, an emission bandwidth less than 0.3 nm can be achieved, which is three order of magnitude smaller than the metal metamaterials based thermal emitter counterparts. We also demonstrate that the emission wavelength can be flexibly adjusted to cover a large part of the MIR regime below the phonon resonance of Al_2O_3. Although the results presented in this work are obtained by neglecting the material loss of the Al_2O_3 film, which is valid when some thin film deposition techniques (e.g. the laser pulsed method [26]) are used, we should note that even when some minor loss of Al_2O_3 is considered, e.g. the imaginary part of its permittivity is assumed to be 2×10^{-5}, a Q–factor as high as 3.0×10^4 can be achieved by adjusting the value of δ, much higher than those realized with metallic metamaterial-based thermal emitters. By replacing Al_2O_3 with other low-loss refractory materials, thermal emission with ultra-narrow bandwidth covering the whole IR to even THz band can be realized. We believe that the BIC based thermal emitters provide a simple yet effective approach of realizing superior sources ranging from IR to THz, with the potential to replace the expensive III–V semiconductor based sources and pave the way for the requirement of light sources in a variety of applications, especially sensing where the power level is not important.

Data availability

The data that support this article, and are not published elsewhere as cited, are available from the corresponding author upon reasonable request.

The data that support the findings of this study are available upon reasonable request from the authors.

Funding

National Natural Science Foundation of China (11974221, 11974218, 91750201) and Local science and technology development project of the central government of China (No. YDZX20203700001766).

ORCID iDs

Kaili Sun https://orcid.org/0000-0003-4587-1857
Zhanghua Han https://orcid.org/0000-0002-4177-2555

References

[1] Lochbaum A, Fedoryshyn Y, Dorodnyy A, Koch U, Hafner C and Leuthold J 2017 On-chip narrowband thermal emitter for Mid-IR optical gas sensing *ACS Photonics* **4** 1371–80
[2] Ali M O, Tait N and Gupta S 2018 High-Q all-dielectric thermal emitters for mid-infrared gas-sensing applications *J. Opt. Soc. Am.* A **35** 119–24
[3] Wang L and Mizaikoff B 2008 Application of multivariate data-analysis techniques to biomedical diagnostics based on mid-infrared spectroscopy *Anal. Bioanal. Chem.* **391** 1641–54
[4] Michel A P M, Liakat S, Bors K and Gmachl C F 2013 *In vivo* measurement of mid-infrared light scattering from human skin *Biomed. Opt. Express* **4** 520–30
[5] Yang S, Yan X, Qin H, Zeng Q, Liang Y, Arguello H and Yuan X 2021 Mid-infrared compressive hyperspectral imaging *Remote Sens.* **13** 741
[6] Hermes M *et al* 2018 Mid-IR hyperspectral imaging for label-free histopathology and cytology *J. Opt.* **20** 023002
[7] Andrade J M, Sánchez M S and Sarabia L A 1999 Applicability of high-absorbance MIR spectroscopy in industrial quality control of reformed gasolines *Chemometr. Intell. Lab. Syst.* **46** 41–55
[8] Dinh T V, Choi I Y, Son Y S and Kim J C 2016 A review on non-dispersive infrared gas sensors: improvement of sensor detection limit and interference correction *Sens. Actuators* B **231** 529–38
[9] Tan X, Zhang H, Li J, Wan H, Guo Q, Zhu H, Liu H and Yi F 2020 Non-dispersive infrared multi-gas sensing via nanoantenna integrated narrowband detectors *Nat. Commun.* **11** 1–9
[10] Yao Y, Hoffman A J and Gmachl C F 2012 Mid-infrared quantum cascade lasers *Nat. Photon.* **6** 432–9
[11] Bewley W W, Canedy C L, Kim C S, Kim M, Merritt C D, Abell J, Vurgaftman I and Meyer J R 2012 High-power room-temperature continuous-wave mid-infrared interband cascade lasters *Opt. Express* **20** 20894–901
[12] Kawasaki T, Fujioka J, Imai T, Torigoe K and Tsukiyama K 2014 Mid-infrared free-electron laser tuned to the amide I band for converting insoluble amyloid-like protein fibrils into the soluble monomeric form *Lasers Med. Sci.* **29** 1701–7
[13] Baranov D G, Xiao Y, Nechepurenko I A, Krasnok A, Alù A and Kats M A 2019 Nanophotonic engineering of far-field thermal emitters *Nat. Mater.* **18** 920–30
[14] Liu X, Tyler T, Starr T, Starr A F, Jokerst N M and Padilla W J 2011 Taming the blackbody with infrared metamaterials as selective thermal emitters *Phys. Rev. Lett.* **107** 045901
[15] Chan D L C, Soljačić M and Joannopoulos J D 2006 Thermal emission and design in one-dimensional periodic metallic photonic crystal slabs *Phys. Rev.* E **74** 016609
[16] Inoue T, De Zoysa M, Asano T and Noda S 2013 Single-peak narrow-bandwidth mid-infrared thermal emitters based on quantum wells and photonic crystals *Appl. Phys. Lett.* **102** 191110
[17] Greffet J J, Carminati R, Joulain K, Mulet J P, Mainguy S and Chen Y 2002 Coherent emission of light by thermal sources *Nature* **416** 61–64
[18] Guo C, Guo Y, Lou B and Fan S 2021 Wide wavelength-tunable narrow-band thermal radiation from moiré patterns *Appl. Phys. Lett.* **118** 131111
[19] Kats M A, Blanchard R, Zhang S, Genevet P, Ko C, Ramanathan S and Capasso F 2014 Vanadium dioxide as a natural disordered metamaterial: perfect thermal emission and large broadband negative differential thermal emittance *Phys. Rev.* X **3** 041004
[20] Tian J, Li Q, Lu J and Qiu M 2018 Reconfigurable all-dielectric antenna-based metasurface driven by multipolar resonances *Opt. Express* **26** 23918
[21] Friedrich H 1985 Interfering resonances and bound states in the continuum *Phys. Rev.* A **32** 3231–42
[22] Lyapina A A, Maksimov D N, Pilipchuk A S and Sadreev A F 2015 Bound states in the continuum in open acoustic resonators *J. Fluid Mech.* **780** 370–87
[23] Calajó G, Fang Y L L, Baranger H U and Ciccarello F 2019 Exciting a bound state in the continuum through multiphoton scattering plus delayed quantum feedback *Phys. Rev. Lett.* **122** 073601
[24] Marinica D C, Borisov A G and Shabanov S V 2008 Bound states in the continuum in photonics *Phys. Rev. Lett.* **100** 183902
[25] Wan W, Yang X and Gao J 2016 Strong coupling between mid-infrared localized plasmons and phonons *Opt. Express* **24** 12367
[26] Boidin R, Halenkovič T, Nazabal V, Beneš L and Němec P 2016 Pulsed laser deposited alumina thin films *Ceram. Int.* **42** 1177–82
[27] Kirchhoff G 1860 I. On the relation between the radiating and absorbing powers of different bodies for light and heat *London, Edinburgh Dublin Phil. Mag. J. Sci.* **20** 1–21
[28] Han Z, Ding F, Cai Y and Levy U 2021 Significantly enhanced second-harmonic generations with all-dielectric antenna array working in the quasi-bound states in the continuum and excited by linearly polarized plane waves *Nanophotonics* **10** 1189–96
[29] Liu B, Gong W, Yu B, Li P and Shen S 2017 Perfect thermal emission by nanoscale transmission line resonators *Nano Lett.* **17** 666–72
[30] Inoue T, De Zoysa M, Asano T and Noda S 2016 On-chip integration and high-speed switching of multi-wavelength narrowband thermal emitters *Appl. Phys. Lett.* **108** 091101
[31] Inoue T, De Zoysa M, Asano T and Noda S 2018 Wavelength-switchable mid-infrared narrowband thermal emitters based on quantumwells and photonic crystals *IEICE Trans. Electron.* **E101C** 545–52
[32] Wiersig J 2006 Formation of long-lived, scarlike modes near avoided resonance crossings in optical microcavities *Phys. Rev. Lett.* **97** 253901